

STADA: Specification-based Testing for Autonomous Driving Agents

Joy Saha¹, Trey Woodlief², Sebastian Elbaum¹, and Matthew B. Dwyer¹

Abstract—Simulation-based testing has become a standard approach to validating autonomous driving agents prior to real-world deployment. A high-quality validation campaign will exercise an agent in diverse contexts comprised of varying static environments, e.g., lanes, intersections, signage, and dynamic elements, e.g., vehicles and pedestrians. To achieve this, existing test generation techniques rely on template-based, manually constructed, or random scenario generation. When applied to validate formally specified safety requirements, such methods either require significant human effort or run the risk of missing important behavior related to the requirement.

To address this gap, we present STADA, a Specification-based Test generation framework for Autonomous Driving Agents that systematically generates the space of scenarios defined by a formal specification expressed in temporal logic (LTL_f). Given a specification, STADA constructs all distinct initial scenes, a diverse space of continuations of those scenes, and simulations that reflect the behaviors of the specification.

Evaluation of STADA on a variety of LTL_f specifications formalized in SCENEFLOW using three complementary coverage criteria demonstrates that STADA yields more than $2\times$ higher coverage than the best baseline on the finest criteria and a 75% increase for the coarsest criteria. Moreover, it matches the coverage of the best baseline with 6 times fewer simulations. While set in the context of autonomous driving, the approach is applicable to other domains with rich simulation environments.

I. INTRODUCTION

The development of autonomous vehicles (AVs) is progressing rapidly with projections that tens of thousands of commercial AVs will be deployed in the coming years [1]. Like human drivers, these systems must adhere to rules of safe driving, e.g., coming to a complete stop at a stop sign, maintaining a safe following distance, or maintaining a safe distance when overtaking another vehicle. Researchers [2], [3], [4], [5] have developed promising methods for specifying such properties using pre and postconditions. Here, the precondition defines the context for a driving rule, such as the spatial and temporal relationship of vehicles at an intersection, and the postcondition states allowable AV behavior in that context, like yielding the right-of-way.

Validating an AV’s adherence to such properties requires constructing a scenario that meets the precondition. For example, the scenario must show that as the *ego* vehicle (the vehicle whose behavior is specified by the property) approaches the intersection other vehicles are already there, thereby establishing the context within which the *ego* vehicle’s behavior can be judged against the postcondition, i.e., whether it yields to the other vehicles or not. Constructing

such scenarios is the crux of testing AV agents, and it is typically performed using simulators like CARLA [6].

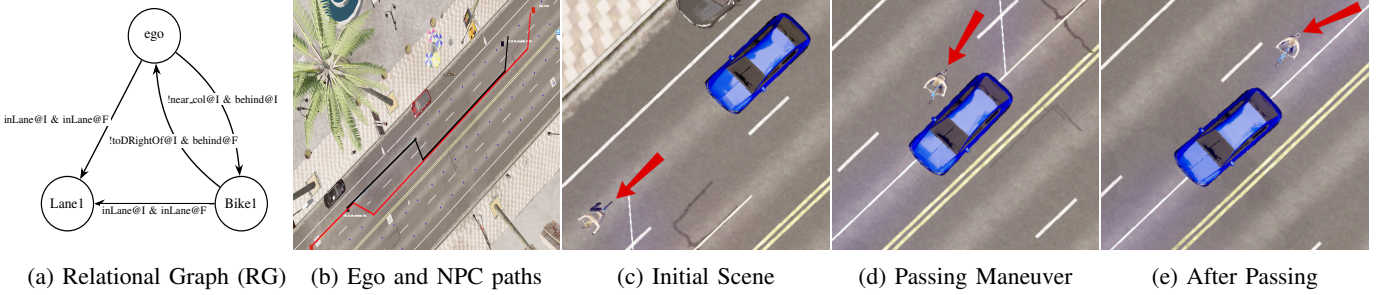
Existing methods for performing such simulation-based property validation fall into two categories. Techniques may develop a fixed set of scenarios [7], [8] or leverage crash data to reconstruct test scenarios [9], [10] to produce tests that meet the precondition. However, there may be multiple ways to establish the precondition, e.g., different timings and numbers of vehicles arriving at an intersection, and this prior work does not explore this diversity. In contrast, fuzzing using algorithmic [11] or LLM-based approaches [12], [13] can produce large, and potentially diverse sets of tests, but those tests may fail to meet the particular precondition rendering them of little value for validating a target property.

In this paper, we develop an automated approach to *Specification-based Testing for Autonomous Driving Agents* (STADA). STADA builds on SCENEFLOW [3] specifications that describe temporal relationships, using LTL_f [14], between states of a system that are described by spatial relationships among objects in a scene. Figure 1 shows a SCENEFLOW specification, φ , of an overtaking maneuver of a *non-player character* (NPC) – a simulation entity not controlled by the agent under test. The precondition (shown in blue) requires that the *ego* vehicle is behind (*behind_bike*) and at a safe distance (*bike_safe_distance*) from a bike, and in the future it is in front of the bike (*in_front_bike*). These atomic propositions are defined using relational logic over a scene graph (SG) computed from sensor inputs, e.g., $behind_bike \equiv ego.aheadOf \cap Bike \neq \emptyset$. The test generation challenge is to configure simulation environments that bias the agent controlling the *ego* to meet this precondition, after which the post-condition can be checked, e.g., that a safe distance is maintained through the maneuver.

To achieve this, as depicted in Figure 1, STADA analyzes the LTL_f structure of the specification and defines a set of *relational graphs* (RG) that contain distinct scenarios that meet the precondition (1.a). These graphs encode requirements both on the initial state in the scenario (1.c) and on the trajectories through the environment established by that initial state. STADA computes the space of trajectories consistent with the precondition (1.b) and selects a diverse subset of those for simulation. The initial state and trajectories are used to generate simulation code that establishes the initial state (1.c) and then biases the *ego*’s agent towards meeting intermediate (1.d) and final (1.e) states corresponding to the precondition.

We implemented STADA using the SCENIC [15] language to generate the initial scene and Python to generate CARLA [6] simulations. An evaluation using two different

¹University of Virginia, Virginia, USA {daa7mv, selbaum, matthewbdwyer}@virginia.edu ²William & Mary, Virginia, USA woodlief@wm.edu



$$\varphi \equiv (\text{behind_bike} \wedge \text{bike_safe_distance} \wedge \mathbf{F}(\text{in_front_bike})) \Rightarrow \mathbf{X}(\text{bike_safe_distance} \cup \text{in_front_bike})$$

Fig. 1: (a) Relational graph for the precondition of φ shown in blue. (b) The ego (red) and NPC (black) paths. (c) Initial scene satisfies *behind_bike* and *bike_safe_distance* (*in_front_bike* pending). (d) During passing, *bike_safe_distance* is violated. (e) After passing, *in_front_bike* is satisfied. The NPC bike is marked with a red arrow and the ego is a blue car.

driving agents and comparing against three baseline techniques shows that STADA is cost-effective in automating the generation of diverse simulations that are consistent with temporal-logic driving properties. It yields more than twice the coverage of the space of precondition-consistent behaviors than the best baseline technique and can match the coverage of those techniques in 6 times fewer simulations. We describe the STADA approach in Section III, its evaluation in Section IV, and background and related work next.

II. RELATED WORK AND BACKGROUND

We briefly survey related work on coverage, test generation, and property specification and monitoring for AVs and provide relevant background on SCENIC and SCENEFLOW.

A. Coverage and Test Generation for AVs

The test adequacy problem aims to determine whether a test suite sufficiently exercises a given system under test (SUT), typically defined through a *coverage criteria*. Prior work in the AV space has measured coverage for system-level testing based on the number of *scenarios of interest* that are covered [16], where the scenario universe is defined using features such as the road structure [17] or vehicle interactions [18]. Specification-based testing evaluates an SUT with respect to its formal specifications to increase confidence in correctness [19], [20]. Prior work on AV test coverage proposed Spatial Semantic Scene Coverage, which used specifications to define a coverage domain based on individual scenes [21]. STADA extends this by supporting test generation and coverage of *temporal* specifications.

Prior work has also proposed test generation techniques, including automated methods such as random [21] or coverage-based scenario generation [17], [18], and manual methods which encode specific scenarios of interest to ensure coverage of, e.g., prior crash scenarios [22]. Tools such as SCENIC, a probabilistic scenario description language, are used to describe AV test cases capable of capturing rich scenes and dynamic behaviors [15] and have been used to convert natural language crash scenarios into operable tests [23]. We built on this tool and use it as a baseline.

While prior approaches measure coverage or generate scenarios, they do not leverage spatial-temporal specifications to systematically generate tests and measure coverage.

B. Specifying AV Properties

To systematically generate test inputs from specifications, AV safety requirements must be formalized in a logic that encodes environmental aspects using primitives that preserve their physical semantics.

Prior work on runtime monitoring for AVs has used Relational First-Order Logic (RFOL) over scene graphs (SGs) [2], [3] to express robust and diverse specifications. The vertices of an SG represent entities in a scene, and the edges represent spatial relationships between entities. RFOL expressions describe sets of SG vertices, using operators $\{\cup, \cap, \setminus, \Delta\}$; the relational image operator, $S.r$, which computes the set of vertices reachable using a designated relation, r , starting with any vertex in a given set, S . Resulting sets can be queried to determine their size, $|S|$, and this can be used, for example, to express non-emptiness, $|S| > 0 \equiv S \neq \emptyset$.

While RFOL captures spatial relationships at a single time instant, AV safety requirements also specify how these relationships evolve over time. To support this, Linear Temporal Logic over Finite Traces or LTL_f [14] is used to express finite-horizon, discrete-time specifications that are well-suited for AV safety requirements. LTL_f contains the temporal operators globally, $\mathbf{G}(\varphi)$, eventually, $\mathbf{F}(\varphi)$, next, $\mathbf{X}(\varphi)$, and until, $(\varphi_1)\mathbf{U}(\varphi_2)$. Prior work has demonstrated the utility of LTL_f to express safe driving requirements in runtime monitoring [2], [3]. This is enabled by the fact that an LTL_f specification translates to a deterministic finite automaton (DFA) which can be used to efficiently determine whether a trace meets the specification [24].

SCENEFLOW specifications [3] combine atomic propositions (APs) built from RFOL over scene graphs, e.g., capturing that the ego's lane is controlled by a stop sign, and LTL_f , e.g., specifying the temporal sequence of stopping, waiting, and proceeding from the stop sign when clear.

In this work, in contrast to other test generation techniques, STADA leverages this structured specification framework

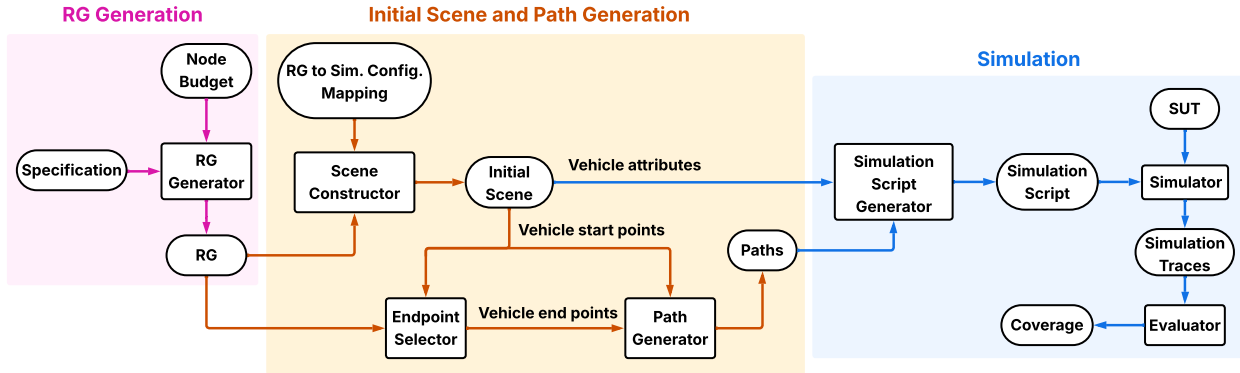


Fig. 2: Overview of STADA.

for systematic test input generation. STADA uses the individual RFOL APs to constrain the space of *scenes* to consider and the LTL_f to constrain the temporal evolution of the *scenario* to guide test generation based on the specification.

SCENEFLOW specifications, $\varphi = \varphi_{pre} \rightarrow \varphi_{post}$, can be decomposed into precondition, φ_{pre} , and postcondition, φ_{post} , pairs. If a specification cannot be decomposed into this form, STADA uses the full specification φ to bias test generation towards relevant scenarios. Since φ_{pre} describes a condition that is initially false and that becomes true at some point in a trace, it will typically not contain the \mathcal{G} operator. STADA assumes preconditions are \mathcal{G} -free in Section III-C.

III. APPROACH

As a specification-based testing approach, STADA aims to *cover* the different ways a system can satisfy the specification. To achieve this for LTL_f preconditions, STADA must address the fact that both the LTL_f formula and the RFOL expressions defining atomic predicates (APs) symbolically encode an enormous space of system behavior.

A. Key Insight

Consider the precondition expressing a vehicle to the left of or behind the *ego*, and in the future a car in front of it:

$$|ego.left \cup ego.behind| > 0 \wedge F(|ego.aheadOf \cap Car| > 0)$$

where *ego* is the singleton set defining the vehicle under test, $\{left, behind, aheadOf\}$ are relations, and *Car* is the set of cars. This might be used to capture the notion of the *ego* being passed by a car, allowing for the position of the passing car to evolve from being behind, then on the left, then in front, over time. While capturing this intent, the precondition specification allows for an enormous variety of traces to satisfy it. For example, such sequences could forgo ever being behind the *ego* by just overtaking in the left lane, or being behind and passing on the right, and there may be cars both behind and to the left. The generality of RFOL and LTL_f in capturing behavior is its strength, but it presents challenges in determining how many different *configurations* of the simulation are required for exploring the diversity present in the precondition.

To address this, STADA leverages the fact that the traces generated from a finite simulation are bounded. Moreover, as described in Section II, LTL_f behavior can be encoded as the finite traces accepted by a deterministic finite state machine. This scoping of behavior allows STADA to define the structure of disjoint configurations that collectively cover the behavior of an LTL_f precondition. These configurations can be used to generate initial scenes of simulations and paths for establishing conditions that aim to drive those simulations towards the goal of meeting the preconditions.

B. Approach Overview

STADA consists of three modules as depicted in Figure 2. The inputs to the framework consist of (i) the precondition of a safe-driving specification expressed in LTL_f , and (ii) a *node budget* defining the number of entities for each node type referenced in the specification. A minimum budget ensures coverage of precondition scenarios, while increasing the budget allows for more and more diverse tests to be generated. The process begins with the generation of a set of relational graphs (RGs) by the **RG Generation** module, each of which represents a distinct system behavior of satisfying the precondition. For each such RG, the **Initial Scene and Path Generation** module generates a static initial scene that satisfies the initial conditions, including spatial, topological, and placement constraints, and then generates feasible paths for the ego and all other relevant entities in the scene, i.e., the NPCs. The **Simulation** module integrates the initial scene and paths to run simulations using the SUT controlling the ego and the Evaluator checks the resulting simulation traces against the LTL_f , which enables postcondition evaluation upon precondition satisfaction.

C. RG Generation

Figure 2 first shows the **RG Generation** module, which analyzes an LTL_f specification to identify all of the ways its precondition can be satisfied. It decomposes the specification into configurations, which are distinct sets of choices that together cover all scenarios consistent with the precondition.

The generator begins by preprocessing the LTL_f formulas. First, operators like implication are converted to

negation, conjunction, and disjunction. Second, disjunctions $\varphi_1 \vee \varphi_2$ are split into three mutually exclusive cases: (i) $\varphi_1 \wedge \neg\varphi_2$, (ii) $\neg\varphi_1 \wedge \varphi_2$, and (iii) $\varphi_1 \wedge \varphi_2$. This results in a set of conjunction-only formulas, which the RG generator processes independently.

The RG generation aims to produce a set of configurations, each of which is defined as a relational graph: $RG = (V, E, L_E)$, where V contains nodes corresponding to the entity types referenced in the specification, and $E \subseteq V \times V$ are edges. The labeling function $L_E : E \mapsto R@T$ maps edges to a relation R and a temporal operator $T \in \{\mathbf{I}, \mathbf{X}, \mathbf{F}, \mathbf{U}_l, \mathbf{U}_r\}$. Here, we introduce \mathbf{I} to define constraints for initial states, the unary temporal operators \mathbf{X}, \mathbf{F} annotate edges with constraints, and the binary operator \mathbf{U} is modeled by pairs of edges with constraints for the left and right operands. For example, an edge labeled $R@\mathbf{F}$ from s to t implies that eventually $t \in s.R$. Binary operators like ‘‘Until’’ (\mathbf{U}) are modeled via pairs: $R_1@\mathbf{U}_l$ and $R_2@\mathbf{U}_r$ represent $(t_1 \in s_1.R_1)\mathbf{U}(t_2 \in s_2.R_2)$. If a temporal operator is missing from an AP, it defaults to \mathbf{I} (Initially).

The process starts with a relational graph G containing only the ego node and iteratively refines it to satisfy each AP_i in the specification. For each AP_i , as depicted in Algorithm 1, the algorithm first decomposes AP_i into a set of (src_j, rel_j, τ) tuples using all the relational image operators referenced in the RFOL expression and extends G with additional nodes of type τ up to the predefined node budget, where τ denotes the vertex type of elements in the set computed by the RFOL expression in AP_i . It then enumerates all ordered tuples (S_1, \dots, S_m) where each S_j is a subset of the candidate node set \mathcal{D} , i.e., it explores the Cartesian product $\mathcal{P}(\mathcal{D})^m$ and adds edges (src_j, rel_j, v) for all $v \in S_j$, thereby generating candidate RG set for AP_i . Only graphs satisfying consistency checks (e.g., a vehicle cannot be simultaneously ahead of and behind another) are passed to the next iteration. Failing to find at least one satisfiable graph at any iteration, the algorithm returns no solution, indicating that the LTL_f formula is not satisfiable within the given node budget. The final output of this module is a set of structurally unique RGs, obtained after removing isomorphic duplicates, each of which satisfies the precondition in a distinct way.

D. Initial Scene and Path Generation

As depicted in Figure 2, the Scene Constructor takes a relational graph (RG) and its corresponding simulation mappings to generate a simulation scene. By leveraging a scene construction tool (e.g., SCENIC, OpenSCENARIO [25]), it then instantiates an initial static scene in a simulator’s native language. Formally, using the given mapping \mathcal{M} and the RG , the Scene Constructor produces a simulator scene Σ and instantiates it using a scene construction tool \mathcal{E} , getting an initial scene \mathcal{X} : $\mathcal{M} : RG \rightarrow \Sigma$ and $\mathcal{E} : \Sigma \rightarrow \mathcal{X}$. This initial scene captures the poses of the ego as well as the NPCs, and the generated coordinates serve as markers for the subsequent path generation.

Algorithm 1 Candidate RG Generation for an AP

```

1: Input: Initial graph  $G$ , Atomic Proposition  $AP_i$ 
2: where  $AP_i = \{(src_j, rel_j, \tau) \mid 1 \leq j \leq m\}$ 
3: Output: Set of candidate RGs  $\mathcal{C}$ 
4:  $n \leftarrow NodeBudget(\tau) - |\{v \in G \mid type(v) = \tau\}|$ 
5: Add  $n$  new nodes of type  $\tau$  to  $G$ 
6:  $\mathcal{D} \leftarrow \{v \in G \mid type(v) = \tau\}$ 
7:  $\mathcal{C} \leftarrow \emptyset$ 
8: for all  $(S_1, \dots, S_m) \in \mathcal{P}(\mathcal{D})^m$  do
9:    $G' \leftarrow$  copy of  $G$ 
10:  for  $j = 1$  to  $m$  do
11:    for all  $v \in S_j$  do
12:      Add edge  $(src_j, rel_j, v)$  to  $G'$ 
13:    end for
14:  end for
15:  Remove all  $v \in \mathcal{D}$  where  $deg(v) = 0$  in  $G'$ 
16:   $\mathcal{C} \leftarrow \mathcal{C} \cup \{G'\}$ 
17: end for
18: return  $\mathcal{C}$ 

```

Once the initial poses are identified, the module generates routes that are consistent with the scene. This is achieved through a two-stage process designed to bias trajectories toward satisfying a target RG. First, the module identifies the trajectories’ endpoints for the vehicles. It binds RG concepts like lane and intersection nodes to concrete road entities in the simulator’s road network. In cases where the binding cannot be unequivocally established, the module defaults to a valid entity. Then, to determine the final destination for each vehicle, it samples a set of simulator waypoints within an initial radius r of the starting point, it filters that set based on the RG edges (e.g., to the side, behind). If the filter returns an empty set, the radius r is increased, and the space is resampled until a feasible set of endpoints is obtained from which one is randomly selected as the final endpoint.

Second, the module constructs a dense waypoint graph onto the scene topology where waypoints are nodes and legal transitions are edges [26]. This higher resolution representation enables the expression of fine-grained behaviors, such as mid-lane changes or overtaking. Then, the module maps the starting and ending positions for the ego and NPCs on this graph to begin trajectory planning. It uses the K-shortest simple path algorithm [27] to find k feasible paths. To increase structural diversity and coverage of maneuvers such as lane changes and positional reordering, the module employs greedy selection, iteratively choosing p^* from the set of candidates \mathcal{O} that maximizes its average distance from the set of already-selected paths \mathcal{L} : $p^* = \arg \max_{p \in \mathcal{O} \setminus \mathcal{L}} \frac{1}{|\mathcal{L}|} \sum_{q \in \mathcal{L}} D(p, q)$ where $D(p, q)$ is the average Euclidean distance between the points of p and q .

E. Simulation

This module receives the vehicle attributes (e.g., vehicle models) and the paths for all vehicles from the **Initial Scene and Path Generation** module, and, using the Simulation Script generator, produces an executable simulation script that spawns the vehicles at the starting positions of their paths and assigns driving controllers to them. The ego is

controlled by the system under test (SUT), while all NPCs are driven using driving agents on autopilot.

We assume that the only externally controllable parameter for the SUT is the route. For the NPC, the module can control steering angle, throttle, speed, and the route. Since the NPC speed is a key variable that can directly influence the precondition satisfaction, and keeping it constant for all specifications would be insufficient to generalize effectively, we leverage the fact that most of the traffic laws tend to trigger if the ego and the NPCs are within close proximity. As such, we dynamically update the speed of the NPCs at each simulation step by decreasing it if the NPC is ahead of the ego and increasing it if it is behind the ego, so that they tend to stay closer to each other. Additionally, the amount of speed change is proportional to the distance between the vehicles. We use the longitudinal separation between the vehicles instead of the Euclidean distance because lateral distance should not influence speed change.

$$v_{\text{npc}}(d) = \text{clip}(v_0 + (\alpha \mathbf{1}_{d \geq 0} - \beta \mathbf{1}_{d < 0})d, v_{\text{min}}, v_{\text{max}}) \quad (1)$$

where d represents the longitudinal deviation, v_0 is the nominal NPC speed, α and β are proportional gain parameters, and v_{min} and v_{max} bound the speed within safe limits. This formulation ensures a smooth, bounded as well as a distance-proportional speed adaptation.

Using the selected agents, paths, and dynamically adjusted speeds, the [Simulation](#) module executes the simulation script and records the trace using a scene graph generator.

Finally, the Evaluator checks the traces against the LTL_f specifications to produce coverage metrics. Disjunctions in an LTL_f define different ways that a precondition may be satisfied, and the presence of multiple forms of disjunction in a precondition induces a combinatorial space of possible configurations to be explored during testing. Conceptually, a configuration defines a combination of choices for each disjunctive fragment of a precondition, e.g., the left or right operands of a \vee in LTL_f or a \cup in RFOL.

The coverage metrics are defined in increasing order of coarseness. The finest-grained metric, cov_1 , measures how many distinct configurations are covered across all simulation traces of a particular treatment. Another metric cov_2 is applicable to a specific class of LTL_f specifications in which multiple APs present in an earlier timestamp are flipped in a later timestamp. We define a *oneflip* configuration as one in which exactly one AP is flipped, and cov_2 specifies how many of these *oneflips* are covered out of all possible *oneflip* cases. This approach is analogous to Modified Condition/Decision Coverage (MC/DC) [28] in structural testing, as it ensures each AP independently affects the outcome. This isolation is critical for detecting edge-case bugs that might be masked if multiple APs always change simultaneously. Finally, cov_3 is a binary coverage metric that checks whether at least one of the distinct configurations mentioned in cov_1 is covered.

IV. EVALUATION

To evaluate the utility of STADA in test input generation for autonomous driving agents, we structure our experiments around the following two research questions:

RQ1: How effective is STADA at generating simulations that cover the space of scenarios in the preconditions of the LTL_f specifications?

RQ2: How efficient is STADA in covering such scenarios?

A. Design

To answer these questions, we require: a set of driving properties in LTL_f , a scene construction tool, a driving simulator, autonomous driving agents as the system under test (SUT), and an evaluator to measure coverage.

For properties, we use the LTL_f specifications defined in SCENEFLOW [3] derived from Virginia Driving Laws. These specifications, shown in Table I, express complex traffic situations, and the language has been shown capable of expressing 110 of 114 (96%) properties in the Regulation of Traffic of the Virginia driving code (Chapter 8) that are applicable to the autonomous driving agent [3].

We use SCENIC [15] as the scene construction tool in STADA. We build an RG-to-SCENIC mapping for each potential relation of the RG. In some cases, multiple edges together instantiate a single code block, such as `isInIntersection` combined with edges specifying the type of intersection control (e.g., traffic lights, stop signs). The `require` statement in SCENIC enforces a hard constraint on the generated scene. For example, an edge in the RG (*ego*, *near*, *car₁*) with *time* = *I* can be expressed in SCENIC by the statement `require (10 < distance from ego to car1 <= 16)` to enforce that in the initial scene the *ego* vehicle must be within 10 to 16 meters of *car₁*, matching the precise semantics of the *near* relation. Distance and angular relationships in this mapping follow the definitions and physical semantics established in prior work [26]. As shown in Section III-D, given a list of parameters such as town, weather, etc., and this mapping \mathcal{M} , the *Initial Scene and Path Generation* module iterates through each edge of the RG and incrementally builds a complete SCENIC program Σ .

We use the popular CARLA 0.9.15 [6] as the simulator, which has diverse road networks, realistic physics simulations, and compatibility with SCENIC. For our experiments, we use the optimized version of *Town10HD* as the map since it has all the necessary road topologies to meet the preconditions in Table I, and *ClearNoon* as the weather running at 20Hz.

Following previous studies [2], [3], we choose Interfuser and Transfuser++ [29] as our two SUTs since they were the best performing agents in CARLA Leaderboard 1 and 2 [30], with available code and model weights. The NPCs are controlled by the CARLA Basic Agent, which allows them to follow a predefined path independent of traffic law.

SCENEFLOW [3] can determine the satisfaction of an LTL_f specification over a set of finite traces generated by

TABLE I: Preconditions of the SCENEFLOW specifications [3] in natural language and the corresponding LTL_fs.

φ_0	If another vehicle arrives at an uncontrolled intersection before the ego and both are later present at the intersection simultaneously , then ... ($atInter(veh, J) \wedge \neg atInter(ego, J) \wedge hasStop(ego)$) \wedge $\mathbf{X}(atInter(veh, J) \wedge atInter(ego, J))$
φ_1	If the ego and another vehicle approach an intersection and, in the next step, are at the intersection with the other to the right , then ... ($\neg atInter(veh, J) \wedge \neg atInter(ego, J) \wedge hasStop(ego) \wedge hasStop(veh)$) \wedge $\mathbf{X}(atInter(veh, J) \wedge atInter(ego, J) \wedge toRightOf(ego, veh))$
φ'_1	If the ego and another vehicle approach an intersection and are at the intersection at some future time with the other to the right , then ... ($\neg atInter(veh, J) \wedge \neg atInter(ego, J) \wedge hasStop(ego) \wedge hasStop(veh)$) \wedge $\mathbf{F}(atInter(veh, J) \wedge atInter(ego, J) \wedge toRightOf(ego, veh))$
φ_2	If an emergency vehicle with lights on is present at a signaled intersection while the ego is entering there , then ... $\neg atInter(ego) \wedge \mathbf{X}(atInter(veh, J) \wedge hasEmergencyLights(veh) \wedge atInter(ego, J) \wedge notEqual(veh, ego))$
φ_3	If the ego is following another vehicle while the lead vehicle is moving , then ... $\neg(tooClose(ego, veh) \wedge sameLane(veh, ego) \wedge behind(ego, veh)) \wedge \neg stopped(veh) \wedge$ $\mathbf{X}(tooClose(ego, veh) \wedge sameLane(veh, ego) \wedge behind(ego, veh) \wedge \neg stopped(veh))$
φ_4	If the ego is following an emergency vehicle with sirens on , then ... $\neg(tooCloseToEmergency(ego, veh) \wedge sameLane(veh, ego) \wedge behind(ego, veh)) \wedge isEmergencyVehicle(veh) \wedge$ $\mathbf{X}(tooCloseToEmergency(ego, veh) \wedge sameLane(veh, ego) \wedge behind(ego, veh) \wedge isEmergencyVehicle(veh))$
φ_5	If the ego overtakes a bicycle , then ... ($behind(ego, bike) \wedge safeDistance_D(ego, bike)$) \wedge $\mathbf{F}(behind(bike, ego))$
φ_6	If the ego intends to move into the opposing lane to overtake another vehicle , then ... ($behind(ego, veh) \wedge opposingClear(ego, \ell) \wedge onlyIn(ego, \ell)$) \wedge $\mathbf{F}((front(ego, veh) \wedge onlyIn(ego, \ell)))$
φ_7	If the ego enters an intersection from a given lane , then ... $onlyIn(ego, \ell_1) \wedge \mathbf{X}(fullyInInter(ego)) \wedge \mathbf{X}(\mathbf{X}((fullyInInter(ego) \wedge \neg onlyIn(ego, \ell_2)) \mathbf{U} onlyIn(ego, \ell_2)))$

the CARLA Scene Graph Generator [26], which we use as the Evaluator from Section III-E. Using the decomposition of $\varphi = \varphi_{pre} \rightarrow \varphi_{post}$ discussed in Section II-B, SCENEFLOW can evaluate whether the precondition was met using φ_{pre} and further evaluate the test itself using φ .

B. Treatments

To the best of our knowledge, no existing approach can generate test inputs for autonomous driving agents directly from LTL_f. Only a few tools are capable of generating test inputs or scenarios from a natural language description, but most lack publicly available or fully functional implementations [12], [13]. Nonetheless, we present 4 treatments for our experiments: two stochastic-placement baselines, a state-of-the-art SCENIC scenario generation technique, and STADA.

To target each RG, we run CARLA by spawning the ego and the same number of NPCs as specified in the STADA RG at random locations. Each such configuration is executed the same number of times as STADA, with the ego controlled by the SUT and NPCs by the CARLA Basic Agent. We denote this baseline as **CARLA**_{base}. We create another similar baseline with 10 times more vehicles than **CARLA**_{base}. We include this **CARLA**_{10×} baseline to explore how well-resourced brute force exploration performs.

We use ScenicNL [23], which generates SCENIC code from natural language (NL) scenario descriptions as a third baseline. For each LTL_f a manually written scenario description is provided to ScenicNL as a prompt along with 3 example SCENIC programs and their NL descriptions. These few-shot examples collectively contain at least one instance of all boolean and temporal operators and specifiers required

for expressing any of our target specifications. We use *GPT-4-0613* as the LLM backbone and prompt ScenicNL once for each LTL_f to generate the SCENIC code.

For STADA, we generate two initial scenes for each RG and execute each initial scene with two different paths, generating 4 simulations for each RG. Across the 20 RGs (excluding φ'_1) for the specifications in Table I, this gives a total of 80 simulations. We choose to generate two initial scenes and two paths per scene to minimally validate our framework’s ability to produce multiple valid and diverse instantiations at the initial scene and path generation stages.

We execute each baseline 80 times using randomly generated paths. However, ScenicNL produces only 3 compilable codes out of the 8 LTL_f specifications. Here, if STADA generates n simulations for φ_i , we run the corresponding ScenicNL program n times as well. In total, this results in 36 simulations, and the remaining 44 are considered empty.

C. RQ1: Coverage Results

Table II presents the coverage of the specifications across all treatments. Overall, under cov_1 STADA achieves the highest coverage at 12/15 (80%) for both agents, outperforming both versions of **CARLA**_{10×} (5/15; 33%) by 47 percentage points (pp), **CARLA**_{base} (transfuser) (2/15; 13%) by 67 pp, **CARLA**_{base} (interfuser) (3/15; 20%) by 60 pp, ScenicNL (transfuser) (2/15; 13%) by 67 pp and ScenicNL (interfuser) (1/15; 6%) by 74 pp. Similarly, STADA significantly outperformed all other treatments under both cov_2 and cov_3 . This strong performance demonstrates STADA’s ability to automatically generate tests that cover the preconditions of a complex set of specifications. We discuss the test

Spec. (Feasible RG/ Total RG)	TransFuser												InterFuser											
	CARLA _{base}			CARLA _{10×}			ScenicNL (few-shot)			STADA			CARLA _{base}			CARLA _{10×}			ScenicNL (few-shot)			STADA		
	cov ₁	cov ₂	cov ₃	cov ₁	cov ₂	cov ₃	cov ₁	cov ₂	cov ₃	cov ₁	cov ₂	cov ₃	cov ₁	cov ₂	cov ₃	cov ₁	cov ₂	cov ₃	cov ₁	cov ₂	cov ₃	cov ₁	cov ₂	cov ₃
φ_0 (1/1)	0/1	0/1	0/1	1/1	1/1	1/1	0/1	0/1	0/1	1/1	1/1	1/1	0/1	0/1	0/1	1/1	1/1	1/1	0/1	0/1	0/1	1/1	1/1	1/1
φ_1 (1/1)	0/1	0/1	0/1	0/1	0/1	0/1	0/1	0/1	0/1	0/1	0/1	0/1	0/1	0/1	0/1	0/1	0/1	0/1	0/1	0/1	0/1	0/1	0/1	0/1
φ'_1 (1/1)	0/1	0/1	0/1	0/1	0/1	0/1	0/1	0/1	0/1	1/1	1/1	1/1	0/1	0/1	0/1	0/1	0/1	0/1	0/1	0/1	0/1	1/1	1/1	1/1
φ_2 (1/1)	0/1	0/1	0/1	0/1	0/1	0/1	0/1	0/1	0/1	1/1	1/1	1/1	0/1	0/1	0/1	0/1	0/1	0/1	0/1	0/1	0/1	1/1	1/1	1/1
φ_3 (4/7)	1/4	1/3	1/1	2/4	2/3	1/1	1/4	0/3	1/1	4/4	3/3	1/1	2/4	2/3	1/1	1/4	1/3	1/1	0/4	0/3	0/1	4/4	3/3	1/1
φ_4 (4/7)	0/4	0/3	0/1	1/4	1/3	1/1	0/4	0/3	0/1	3/4	3/3	1/1	0/4	0/3	0/1	2/4	2/3	1/1	0/4	0/3	0/1	3/4	3/3	1/1
φ_5 (1/1)	0/1	0/1	0/1	0/1	0/1	0/1	0/1	0/1	0/1	1/1	1/1	1/1	0/1	0/1	0/1	0/1	0/1	0/1	0/1	0/1	0/1	1/1	1/1	1/1
φ_6 (1/1)	0/1	0/1	0/1	0/1	0/1	0/1	0/1	0/1	0/1	0/1	0/1	0/1	0/1	0/1	0/1	0/1	0/1	0/1	0/1	0/1	0/1	0/1	0/1	0/1
φ_7 (1/1)	1/1	1/1	1/1	1/1	1/1	1/1	1/1	1/1	1/1	1/1	1/1	1/1	1/1	1/1	1/1	1/1	1/1	1/1	1/1	1/1	1/1	1/1	1/1	1/1
Total (15/21)	13%	15%	22%	33%	38%	44%	13%	7%	22%	80%	84%	77%	20%	23%	22%	33%	38%	44%	6%	7%	11%	80%	84%	77%

TABLE II: Coverage comparison across coverage types (cov₁–cov₃) for each method and agent under identical settings.

coverage of selected specifications below in more detail.

For φ_0 , ScenicNL repeatedly generated arbitrary intersections rather than stop sign-controlled ones. Since most of the CARLA intersections are controlled by traffic signals, the likelihood of encountering stop signs was inherently low, reducing ScenicNL’s probability of satisfying φ_0 . On the other hand, STADA generated intersections with stop signs in every simulation of φ_0 , illustrating STADA’s fine-grained control over object attributes, which is particularly impactful when the required attributes are rare.

φ_1 is time-sensitive, meeting the precondition requires that the vehicles arrive at the intersection simultaneously. Since entering the intersection on the exact same frame is extremely unlikely, none of the treatments cover it within the simulated budget. To relax the simultaneity requirement, we replaced the \mathbf{X} in φ_1 with \mathbf{F} and created φ'_1 to specify that, eventually, instead of the next frame, both vehicles were at the intersection. Formally, at frame n , both vehicles are away from the intersection, and at frame $n+h$, both vehicles are at the intersection with the referenced vehicle positioned on the right of the ego. STADA (transfuser) and STADA (interfuser) cover φ'_1 with minimum values of $h = 3$ and $h = 8$ frames respectively, which correspond to 0.15 and 0.40 seconds at 20 Hz. No other treatment could cover φ'_1 .

For φ_3 and φ_4 , negating the conjunctive constraint that defines *following another vehicle too closely* results in 7 ways to satisfy the specifications, 4 of which are physically realizable. STADA covered (4/4; 100%) for φ_3 and (3/4; 75%) for φ_4 , whereas the best baseline only covered 2/4.

φ_5 and φ_6 are the most challenging preconditions to cover because they require the ego to overtake another vehicle in front of it. Only STADA could cover φ_5 , and no technique could cover φ_6 . For φ_5 , it is sufficient that the ego overtakes a bike on the same lane. However, driving agents like Transfuser and Interfuser typically maintain vehicle-following behavior rather than proactive overtaking. For φ_6 , even though the LTL_f does not mention it explicitly, it requires the ego to overtake another vehicle using the opposing lane, which the SUTs were not trained to do. Thus, even though STADA generates paths over the opposing lane, the agents prioritize safety over path adherence and refrain

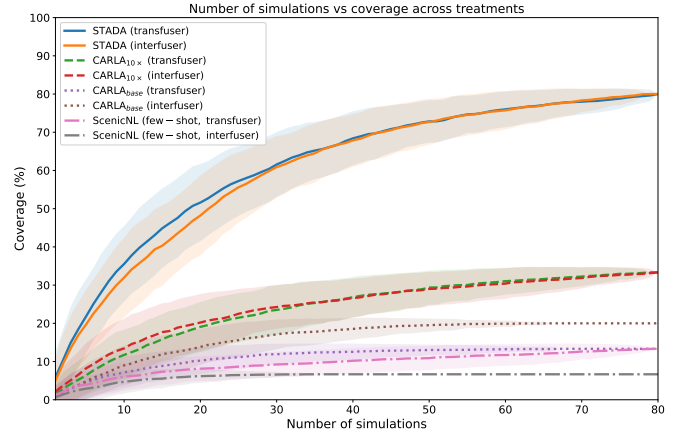


Fig. 3: Mean coverage (cov₁) vs. number of simulations across different treatments.

from overtaking.

Notably, the coverage for STADA and CARLA_{10×} do not vary based on the SUT, while CARLA_{base} and ScenicNL show comparable performance across agents. This is caused by the fact that both SUTs exhibit a similar capability of following trajectory guidance.

Answer to RQ1. STADA is highly effective, producing simulations that cover the LTL_f scenario space, achieving improvements of 47–74 pp in cov₁, 46–77 pp in cov₂, and 33–66 pp in cov₃ over the baselines.

D. RQ2: Efficiency

Figure 3 shows cov₁ as a function of simulation count across different treatments for Transfuser and Interfuser. For each treatment, we sample 200 random permutations of the 80 simulations and compute the mean (lines) and standard deviation (shaded areas) of coverage at each step. STADA rises the fastest and dominates other treatments. Within about 10–12 simulations, STADA passed the second best method CARLA_{10×}’s maximum coverage of 33%. STADA shows a steep initial gain of 50%–55% in the first 20–25 simulations

and steady gains afterwards, demonstrating potential to cover the missing scenarios like the one required for φ_4 . The coverage achieved by CARLA_{10x}, despite having 10 times the entity resources, remains well below STADA, indicating that brute force scaling alone is not sufficient and also sometimes can negatively impact the coverage, e.g., a road that is too crowded can limit lane change possibilities.

Answer to RQ2. STADA is efficient, attaining higher coverage with fewer simulations than competing methods showing plateauing trends.

V. CONCLUSION

This work addresses the question of how to thoroughly test control agents relative to a formal requirement in a realistic simulation environment. STADA achieves this by decomposing LTL_f requirements into a set of graphs that partition its behavior. For each behavior, it generates constraints on the initial scenes and trajectories through the space defined by those scenes that are consistent with the behavior. From this information, it generates simulation code that can be used to instantiate targeted simulations aiming to cover the behavior of the requirements within which agent behavior can be monitored. A broad evaluation across 8 specifications, 3 coverage criteria, and 2 agents under test demonstrates that STADA significantly outperforms 3 state-of-the-art baselines. This provides strong evidence that specification-based test generation for complex temporal requirements can add value to validation processes for autonomous driving agents.

REFERENCES

- [1] “The autonomous vehicle market is forecast to grow and boost ridesharing presence,” 2025, accessed on 09.14.2025. [Online]. Available: <https://www.goldmansachs.com/insights/articles/autonomous-vehicle-market-forecast-to-grow-ridesharing-presence>
- [2] T. Woodlief, F. Toledo, S. Elbaum, and M. B. Dwyer, “The sgsm framework: Enabling the specification and monitor synthesis of safe driving properties through scene graphs,” *Science of Computer Programming*, 2025.
- [3] T. Woodlief, F. Toledo, M. Dwyer, and S. Elbaum, “Scene flow specifications: Encoding and monitoring rich temporal safety properties of autonomous systems,” *Proceedings of the ACM on Software Engineering*, 2025.
- [4] F. Toledo, T. Woodlief, S. Elbaum, and M. B. Dwyer, “T4pc: Training deep neural networks for property conformance,” *IEEE Transactions on Software Engineering*, 2025.
- [5] Y. Sun, C. M. Poskitt, X. Zhang, and J. Sun, “Redriver: Runtime enforcement for autonomous vehicles,” in *Proceedings of the IEEE/ACM 46th International Conference on Software Engineering*, 2024.
- [6] A. Dosovitskiy, G. Ros, F. Codevilla, A. Lopez, and V. Koltun, “Carla: An open urban driving simulator,” 2017. [Online]. Available: <https://arxiv.org/abs/1711.03938>
- [7] H. X. Liu, X. Yan, H. Sun, T. Wang, Z. Qiao, H. Zhu, S. Shen, S. Feng, G. Stevens, and G. McGuire, “Behavioral safety assessment towards large-scale deployment of autonomous vehicles,” 2025. [Online]. Available: <https://arxiv.org/abs/2505.16214>
- [8] Y. Huai, S. Almanee, Y. Chen, X. Wu, Q. A. Chen, and J. Garcia, “scenorita: Generating diverse, fully mutable, test scenarios for autonomous vehicle planning,” *IEEE Transactions on Software Engineering*, 2023.
- [9] S. K. Bashetty, H. B. Amor, and G. Fainekos, “Deepcrashtest: Turning dashcam videos into virtual crash tests for automated driving systems,” 2020. [Online]. Available: <https://arxiv.org/abs/2003.11766>
- [10] R. Zhou, “Efficient safety testing of autonomous vehicles via adaptive search over crash-derived scenarios,” 2025. [Online]. Available: <https://arxiv.org/abs/2508.06575>
- [11] X. Ji, L. Xue, Z. He, and X. Luo, “Autonomous driving system testing via diversity-oriented driving scenario exploration,” 2025. [Online]. Available: <https://doi.org/10.1145/3727875>
- [12] N. Petrovic, K. Lebioda, V. Zolfaghari, A. Schamschurko, S. Kirchner, N. Purschke, F. Pan, and A. Knoll, “Llm-driven testing for autonomous driving scenarios,” in *2024 2nd International Conference on Foundation and Large Language Models (FLLM)*, 2024.
- [13] Y. Mei, T. Nie, J. Sun, and Y. Tian, “Seeking to collide: Online safety-critical scenario generation for autonomous driving with retrieval augmented large language models,” 2025. [Online]. Available: <https://arxiv.org/abs/2505.00972>
- [14] G. De Giacomo and M. Y. Vardi, “Linear temporal logic and linear dynamic logic on finite traces,” in *International joint conference on Artificial Intelligence*. Association for Computing Machinery, 2013.
- [15] D. J. Fremont, T. Dreossi, S. Ghosh, X. Yue, A. L. Sangiovanni-Vincentelli, and S. A. Seshia, “Scenic: a language for scenario specification and scene generation,” in *Proceedings of the 40th ACM SIGPLAN Conference on Programming Language Design and Implementation*. ACM, 2019.
- [16] S. Tang, Z. Zhang, Y. Zhang, J. Zhou, Y. Guo, S. Liu, S. Guo, Y.-F. Li, L. Ma, Y. Xue *et al.*, “A survey on automated driving system testing: Landscapes and trends,” *ACM Transactions on Software Engineering and Methodology*, 2023.
- [17] Y. Tang, Y. Zhou, Y. Liu, J. Sun, and G. Wang, “Collision avoidance testing for autonomous driving systems on complete maps,” in *2021 IEEE Intelligent Vehicles Symposium (IV)*. IEEE, 2021.
- [18] Z. Tahir and R. Alexander, “Intersection focused situation coverage-based verification and validation framework for autonomous vehicles implemented in carla,” in *International Conference on Modelling and Simulation for Autonomous Systems*. Springer, 2021.
- [19] B.-H. Schlingloff and M. Roggenbach, “Specification-based testing,” in *Formal Methods for Software Engineering: Languages, Methods, Application Domains*. Springer, 2022.
- [20] C. Pecheur, F. Raimondi, and G. Brat, “A formal analysis of requirements-based testing,” in *Proceedings of the eighteenth international symposium on Software testing and analysis*, 2009.
- [21] T. Woodlief, F. Toledo, S. Elbaum, and M. B. Dwyer, “S3c: Spatial semantic scene coverage for autonomous vehicles,” in *International Conference on Software Engineering*, 2024.
- [22] E. Thorn, S. C. Kimmel, M. Chaka, B. A. Hamilton *et al.*, “A framework for automated driving system testable cases and scenarios,” United States. Department of Transportation. National Highway Traffic Safety Administration, Tech. Rep., 2018.
- [23] K. Elmaaroufi, D. Shanker, A. Cismaru, M. Vazquez-Chanlatte, A. Sangiovanni-Vincentelli, M. Zaharia, and S. A. Seshia, “Scenic1: Generating probabilistic scenario programs from natural language,” 2024. [Online]. Available: <https://arxiv.org/abs/2405.03709>
- [24] F. Fuggitti, “Ltlf2dfa.”
- [25] ASAM e.v., “OpenSCENARIO standard,” <https://www.asam.net/standards/detail/openscenario/>, 2020.
- [26] T. Woodlief, F. Toledo, S. Elbaum, and M. B. Dwyer, “Closing the gap between sensor inputs and driving properties: A scene graph generator for carla,” in *International Conference on Software Engineering: Companion Proceedings*. IEEE, 2025, pp. 29–32.
- [27] J. Y. Yen, “Finding the k shortest loopless paths in a network,” *Manage. Sci.*, 1971.
- [28] J. Chilenski and S. P. Miller, “Applicability of modified condition/decision coverage to software testing,” *Softw. Eng. J.*, 1994.
- [29] K. Chitta, A. Prakash, B. Jaeger, Z. Yu, K. Renz, and A. Geiger, “Transfuser: Imitation with transformer-based sensor fusion for autonomous driving,” 2023. [Online]. Available: <https://doi.org/10.1109/TPAMI.2022.3200245>
- [30] “Carla autonomous driving leaderboard,” <https://leaderboard.carla.org/leaderboard/>, CARLA, 2025, accessed: 2025-09-10.